Journal of Dental Research
1–7

DOI: 10.1177/0022034518792048
journals.sagepub.com/home/jdr

Enamel Remineralization with Novel Bioactive Glass Air Abrasion

A.A. Taha[1,2], P.S. Fleming[3], R.G. Hill[1], and M.P. Patel[1]

Abstract

Enamel demineralization or white spot lesions (WSLs) are a frequent complication associated with fixed appliance–based orthodontic treatment. The remineralization potential of a novel fluoride-containing bioactive glass (QMAT3) propelled via an air abrasion system was compared with Sylc glass and artificial saliva on artificially induced WSLs. Thirty extracted human premolars were randomly assigned into 3 groups ($n = 10$) per method of treatment and scanned with optical coherence tomography and noncontact profilometer in the 4 enamel states: sound, demineralized, after glass propulsion, and after immersion in artificial saliva. Knoop hardness testing was also performed. Twenty additional prepared teeth samples were also randomly selected for examination by scanning electron microscopy and energy-dispersive X-ray spectroscopy (2 teeth per technique) under each of the 4 enamel conditions. ^{19}F MAS-NMR (magic angle spinning–nuclear magnetic resonance) was also used to detect the type of apatite formed on the enamel surface. Significant enamel remineralization with surface roughness and intensity of light backscattering similar to that of sound enamel was observed following treatment with QMAT3. In addition, mineral deposits were detected on the remineralized enamel surfaces, forming a protective layer and improving its hardness. This layer was rich in calcium, phosphate, and fluoride; ^{19}F MAS-NMR confirmed the formation of fluorapatite. This finding is particularly beneficial since fluorapatite is more chemically stable than hydroxyapatite and has greater resistance to acid attack. Hence, a promising fluoride-containing bioactive glass for enamel remineralization has been developed, although further clinical evaluation and refinement is required.

Keywords: demineralization, biomaterials, fluoride, orthodontics, minerals, dental

Introduction

White spot lesions (WSLs) were reported in up to 96% of orthodontic patients due to impeded ability to clean teeth effectively in the presence of attachments, resulting in food stagnation and plaque formation (Sangamesh et al. 2011). The roughened surfaces of residual adhesive bonding materials around orthodontic brackets also predispose to bacterial attachment. This is aggravated by the fact that most orthodontic patients are adolescents, who are at increased risk attributed to the susceptibility of newly erupting teeth to acid attack (Mayne et al. 2011; Srivastava et al. 2013).

The use of agents such as casein phosphopeptide–amorphous calcium phosphate has been advanced in recent years as an alternative to fluoride in promoting remineralization (Chambers et al. 2013). However, clinical research gave equivocal results with limited benefit being shown relative to topical fluorides (Beerens et al. 2010; Bröchner et al. 2011). Most recently, a bioactive glass (45S5) was used to remineralize WSLs in gel and paste forms (Taha et al. 2017). Milly et al. (2015) mixed 45S5 powder with polyacrylic acid powder to enhance WSL remineralization, using surface preconditioning with air abrasion followed by application of a bioactive glass paste. However, this approach is laborious and requires multiple steps, and while it induces an improved appearance of lesions, a commensurate increase in surface roughness was also observed (Milly et al. 2015). Hence, there remains a need to improve the properties of the 45S5 glass to facilitate safe removal of residual adhesive bonding materials while promoting remineralization of WSLs.

In previous work, we developed a novel fluoride-containing bioactive glass (QMAT3) with a hardness below that of enamel and 45S5, which can be used in a single step capable of removing adhesive without inducing tangible enamel damage (Taha et al. 2018). The aim of this study was therefore to assess the ability of this novel fluoride-containing bioactive glass (QMAT3) propelled via an air abrasion handpiece to induce WSL remineralization, in comparison with a commercially available 45S5 glass (Sylc) and artificial saliva (AS).

[1]Dental Physical Sciences, Barts and the London School of Medicine and Dentistry, Institute of Dentistry, Queen Mary University of London, London, UK
[2]Department of Paedodontic, Orthodontic and Preventive Dentistry, College of Dentistry, Al-Mustansiriya University, Baghdad, Iraq
[3]Department of Orthodontics, Barts and the London School of Medicine and Dentistry, Institute of Dentistry, Queen Mary University of London, London, UK

Corresponding Author:
A.A. Taha, Dental Physical Sciences, Dental Institute, Barts and the London, Queen Mary University of London, Mile End Road, London, E1 4NS, UK.
Email: a.a.h.taha@qmul.ac.uk

Materials and Methods

Tooth Sample and AS Preparation

Fifty human premolars extracted for orthodontic purposes were selected on the basis of visual observation with an optical stereomicroscope at 4.5× magnification (VWR International Microscope), with ethical approval obtained from the Queen Mary Research Ethics Committee (QMREC 2011/99). The inclusion criteria were as follows: no carious lesions, cracks, or any other defects on the buccal surfaces. Teeth were cleaned and stored in deionized water (DW) in a refrigerator at 4 ± 0.1 °C. Prior to the start of the experiment, the teeth were washed with DW, air-dried, and embedded in plastic moulds filled with cold-cure acrylic resin (Orthocryl) with the buccal surfaces exposed. Thereafter, a polyvinyl chloride tape was placed on the buccal surface, which left a central window (4 × 4 mm). The covered area was used as a reference for later visual comparison between the sound and remineralized surfaces. Finally, these prepared teeth samples were stored in an incubator at 37 ± 0.1 °C until use.

AS was prepared according to accepted protocols (Earl et al. 2010; Mneimne 2014) by dissolving the following reagents: potassium chloride (2.24 g), potassium dihydrogen phosphate (1.36 g), sodium chloride (0.76 g), calcium chloride dihydrate (0.44 g) dissolved in 15 mL of DW to prevent precipitation of calcium, and mucin from porcine stomach (2.2 g; all from Sigma-Aldrich) in 800 mL of DW. The pH of AS was then adjusted to 6.5 by slowly adding a 0.5M solution of potassium hydroxide, which was prepared from potassium hydroxide flakes (Sigma-Aldrich). Finally, the AS was topped with DW until the total volume of the solution reached 1 L. It was then placed into a polyethylene bottle in a fridge at 4 ± 0.1 °C before further use and was used within a week to avoid precipitation of calcium phosphate.

Study Protocol

A bilayer demineralization protocol with 8% methylcellulose gel (Sigma-Aldrich) buffered with a layer of lactic acid solution (0.1 mol/L, pH 4.6; Sigma-Aldrich) for 14 d at 37 °C was used to induce artificial subsurface lesions (WSLs) with an average depth of 70 to 100 μm in 30 prepared teeth samples (Ten Cate et al. 2006; Milly et al. 2015). Thereafter, these samples were randomly assigned into 3 experimental groups (n = 10) based on the remineralization treatment.

An air abrasion handpiece (BA Ultimate Air Polisher; air pressure, 60 psi; nozzle angle, 90°; nozzle tip-enamel surface distance, 5 mm) connected to a dental chair unit was used to propel bioactive glasses on the artificially induced WSLs. A commercially available glass (Sylc; Denfotex Research Ltd) and the novel experimental glass (QMAT3) were used to remineralize the demineralized teeth samples, while the control samples were immersed in DW. The novel glass (QMAT3) had the following composition: SiO_2, 37 mol%; Na_2O, 30 mol%; CaO, 23.9 mol%; P_2O_5, 6.1 mol%; and CaF_2, 3 mol% (Sigma-Aldrich).

Teeth from all 3 groups were subsequently immersed in separate plastic containers containing 50 mL of AS for 24 h within an orbital shaker (IKA KS 4000i Control) at 37°C to mimic the oral environment. Optical coherence tomography (OCT), noncontact profilometry, and Knoop hardness testing were undertaken on sound and demineralized enamel, after glass propulsion and after immersion in AS, on 10 prepared teeth randomly assigned from each group. Further investigations involved 20 prepared samples randomly selected for scanning electron microscopy (SEM) and energy-dispersive X-ray spectroscopy (EDX). Two prepared enamel samples were scanned with each technique under specific conditions: 1) sound, 2) demineralized with the aforementioned protocol, 3) remineralized with only AS, 4) remineralized following Sylc–air abrasion and AS immersion, and 5) remineralized following QMAT3–air abrasion and immersion in AS.

Optical Coherence Tomography

Teeth were scanned (n = 10 per group) with OCT (laboratory custom built) to assess the intensity of the light backscattering from the enamel surface prior to demineralization (sound), after demineralization, after glass propulsion, and after immersion in AS (at 1,325-nm central wavelength, 10-kHz frequency, 15-mW energy, and axial and transverse resolutions at 8 and 10 μm in air, respectively). The scanning beam was oriented perpendicular to the enamel surface (area, 3 mm × 3 mm; scan depth, 3 mm). Five hundred grayscale images (B-scans) were performed and analyzed with image processing Fiji software ImageJ.

Profilometry

A noncontact 3-dimensional white light profilometer (Proscan 2000; Scantron) was used to measure the enamel surface roughness. A standard area (1 mm × 1 mm) within the exposed window (4 mm × 4 mm) was scanned 4 times on 10 teeth within each experimental group: prior to demineralization (sound), after demineralization, after glass propulsion, and after immersion in AS. The operating parameters were as follows: frequency rate, 100 Hz; step size, 0.01 mm; and number of steps, 10.

Knoop Hardness Testing

A Struers Duramin microhardness tester with a Knoop elongated pyramid-shaped diamond indenter (Struers Ltd.) was used (50 g load for 10-s dwell time; 40× air objective lens). The Knoop hardness value was calculated by measuring the length of long-axis (diagonal) indentation. Since the enamel has a convex surface, 3 well-shaped indentations, 200 μm apart, were made and averaged per tooth sample (10 teeth per experimental group per varying state) to minimize discrepancy and to avoid the risk of interferences and crack propagation between indentations.

Scanning Electron Microscopy

SEM images (SEM-FEI Inspect F; Oxford Instruments) were produced per enamel condition ($n = 2$) with an accelerated voltage of 20 kV and a working distance of 10 mm. Before imaging, the tooth sample was rinsed thoroughly with DW, dried at room temperature for 48 h, and then coated with a conductive coating (gold) with an automatic sputter coater (SC7620; Quorum Technologies). Consequently, the teeth could not be used after SEM imaging.

Energy-Dispersive X-ray Spectroscopy

The elemental compositions of the prepared enamel samples ($n = 2$ per enamel state) were identified with EDX (Oxford Instruments; voltage, 20 kV; working distance, 10 mm; spatial resolution, 100 nm; count time, 60 s with weight %). Prior to EDX mapping, each tooth sample was dried at room temperature for 48 h and sputter coated with carbon (Balzers/CED 030; Baltec).

Magic Angle Spinning–Nuclear Magnetic Resonance Spectroscopy

19F magic angle spinning–nuclear magnetic resonance (MAS-NMR; Bruker; 600-MHz, 14.1-T spectrometer; Larmor frequency, 564.5 MHz; spinning condition, 22 kHz) was used to confirm the presence of fluorapatite on the enamel surface of an extracted tooth after propelling QMAT3 via the air abrasion handpiece. Five enamel blocks (~4 mm × 4 mm) were harvested (~1-mm thickness) with a diamond cutting machine (Accutom-5; Struers A/S) and immersed in 50 mL of AS in an orbital shaker (IKA KS 4000i Control) for 24 h at 37 °C. Thereafter, each enamel block was dried and ground to a fine powder. One of the blocks was kept aside (sound enamel surface for scanning), while the others were demineralized. After demineralization, 1 enamel block was kept aside (demineralized enamel surface for scanning); another was immersed in AS alone; and the others underwent air abrasion with the novel QMAT3 or 45S5 (Sylc).

19F MAS-NMR spectra were acquired with a low-fluorine background probe (single-pulse experiment, 30-s recycle duration). The 19F chemical shift scale was referenced with the −120-ppm peak of 1M NaF solution. The spectra were acquired overnight with an accumulation of 256 scans.

Statistical Analysis

Descriptive statistics were calculated with data entered into Microsoft Excel for analysis. Inferential statistical analysis was performed with SPSS 24 (IBM). One-way analysis of variance was used to compare mean differences among groups with a Tukey's honest significance difference post hoc test at a prespecified significance level ($P = 0.05$).

Results

OCT Results

The mean intensity of light backscattering from the tooth surface did not differ significantly among the experimental groups at baseline and following demineralization (Fig. 1). In addition, higher light backscattering intensity values were recorded from demineralized enamel surfaces as compared with their corresponding sound values in each experimental group ($P < 0.001$). After glass propulsion with QMAT3 (QMAT–air abrasion group), a significant reduction in intensity values was observed from the tooth surfaces versus the corresponding values when demineralized ($P = 0.033$). After immersion in AS, a further significant reduction in the intensity values was recorded as compared with the corresponding values after glass propulsion ($P < 0.001$), approximating baseline values ($P > 0.99$). Conversely, the intensity values within the Sylc–air abrasion and control groups remained significantly higher than baseline values ($P < 0.001$).

Profilometry Results

A significant increase in enamel roughness was observed following demineralization as compared with baseline for all experimental groups ($P < 0.001$; Fig. 2). After glass propulsion, the roughness measurements in the Sylc–air abrasion group were significantly higher (3.08 ± 0.08 μm) than their corresponding measurements under sound and demineralized conditions ($P < 0.001$). Conversely, there was a significant reduction in the roughness measurements of the QMAT3–air abrasion group following glass propulsion versus the demineralized state ($P < 0.001$), approximating their corresponding sound measurements ($P > 0.99$). After immersion in AS, no significant differences in roughness values were recorded for all experimental groups as compared with those obtained after glass propulsion ($P = 0.599$ to $P > 0.99$).

Knoop Hardness Testing

No significant differences were observed in Knoop hardness among the experimental groups at baseline and following demineralization (Fig. 3). Following demineralization, hardness values significantly decreased as compared with their corresponding sound values for all experimental groups ($P < 0.001$). After immersion in AS, a significant increase was observed in the hardness values of the Sylc–air abrasion and QMAT3–air abrasion groups versus demineralized states and directly after glass propulsion ($P < 0.001$), suggesting that the glass reacted with AS and enhanced remineralization of WSLs. Additionally, enamel hardness in the QMAT3–air abrasion group was significantly higher than for the Sylc–air abrasion and control groups after immersion in AS ($P < 0.001$), although they did not reach their corresponding baseline values.

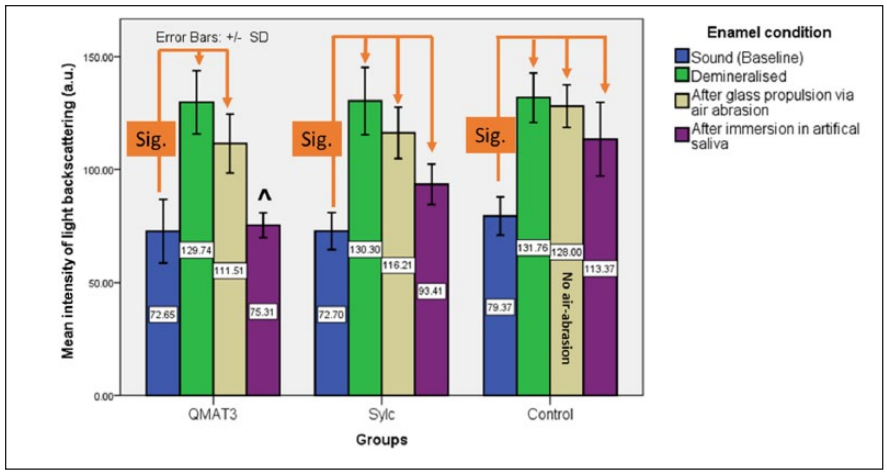

Figure 1. Mean ± SD of the intensity value of light backscattering for each experimental group under 4 conditions.

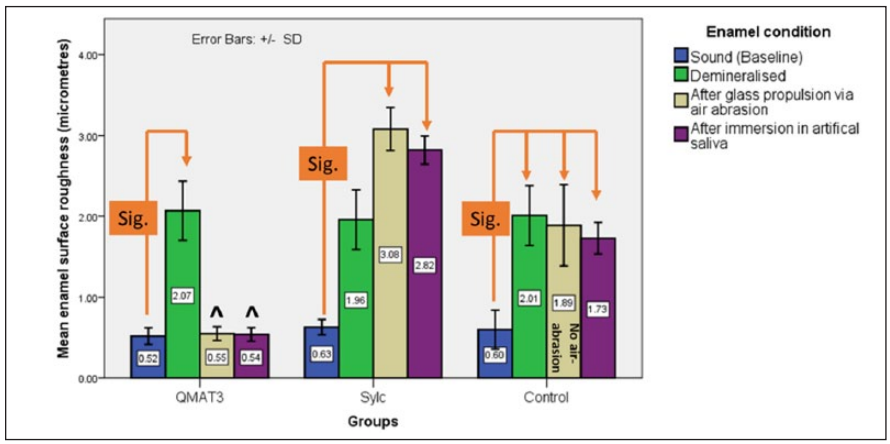

Figure 2. Mean ± SD of the enamel surface roughness in micrometers for each experimental group under 4 conditions.

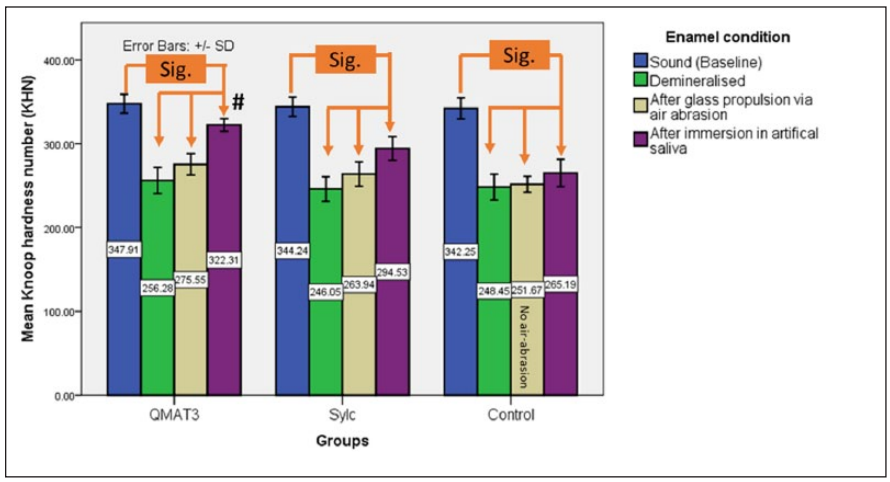

Figure 3. Mean ± SD of Knoop hardness number for each experimental group under 4 conditions.

SEM Results

The sound enamel surface (Fig. 4) appeared homogenous, flat, and smooth, while the demineralized enamel surface appeared rough and porous with voids of variable sizes distributed non-uniformly and with irregular patterns of surface destruction due to the demineralization process. The remineralized enamel surfaces resulting from Sylc–air abrasion and QMAT3–air abrasion were infiltrated by scattered mineral precipitate-like deposits. The latter were more evident and distributed uniformly in QMAT3, completely covering the porosities and resulting in a smoother enamel surface, while these deposits were unevenly distributed on a less uniform enamel surface following Sylc–air abrasion. No evidence of remineralization was observed on the rough enamel surfaces of the control (untreated) group immersed in only AS.

EDX Results

Differences in the emission peaks of some elements, such as Ca, P, O, and Na, were observed in EDX spectra (Fig. 4) of sound and demineralized enamel. In addition, in comparison of the EDX spectra of the remineralized enamel surface in AS alone (control group) with those obtained after remineralization involving glass propulsion (Sylc or QMAT3) and then immersion in AS, an additional peak for silicon (Si) can be seen for Sylc glass at 1.73 keV in the Sylc–air abrasion group. This peak relates to the presence of Sylc glass particles on the enamel surface. Two additional peaks—at 1.73 and 0.65 keV, representing Si and fluoride, respectively—can be seen for QMAT3 glass in the QMAT3–air abrasion group, which indicates embedding of the QMAT3 glass particles into the enamel surface.

Fluorapatite Detection

The ^{19}F MAS-NMR spectra of the enamel surface (Fig. 5) were assessed in 4 states: sound, demineralized, after glass propulsion, and after immersing

in AS to induce remineralization. These appeared as flat lines with no detectable fluoride present in sound and demineralized enamel, when immersed in AS, and after propulsion Sylc glass followed by immersion in AS. Conversely, the enamel surface showed the same characteristic fluorapatite peak at −102 ppm as the fluorapatite reference peak after propulsion of QMAT3 glass followed by immersion in AS.

Discussion

Artificial WSLs were induced in human premolars instead of teeth with natural WSLs, since the latter vary widely in shape, size, and mineral content (Silverstone et al. 1981; Huang et al. 2007; Cochrane et al. 2012). The bilayer demineralization protocol created a subsurface carious lesion with an intact outer surface and depth between 70 and 100 µm. These features were in line with previous studies (Lynch et al. 2007; Magalhães et al. 2009) reporting that lesions induced by bilayer demineralization approximated those of natural lesions.

Kang et al. (2012) found that the porous demineralized enamel surfaces had high-intensity light backscattering due to the increased number and size of pores. Conversely, the light associated with sound and remineralized enamel surfaces is scattered from well-ordered prism structures, resulting in less time for the light to travel within the enamel structure and leading to low-intensity values (Jones and Fried 2006; Milly et al. 2014; Milly et al. 2015). After glass propulsion and immersion in AS, the QMAT3–air abrasion group presented with lower light intensity backscattering values on remineralized enamel surfaces as compared with those obtained for the Sylc air abrasion and control (untreated) groups. This may be due to evenly distributed and profusely scattered QMAT3 glass particles forming a new mineral layer on enamel that fully covered the porous lesion, as observed in SEM images, while Sylc glass particles diffused unevenly on the remineralized enamel surfaces.

Profilometry confirmed higher enamel surface roughness as compared with sound enamel following Sylc propulsion. This may relate to the hardness of this glass (4.6 GPa), which exceeded that of enamel (3.5 GPa). Conversely, due to the lower hardness of QMAT3 (3.4 GPa; approximating but not exceeding that of the enamel surface), the surface roughness of previously demineralized enamel was significantly reduced after propulsion, being similar to that of sound enamel. These findings are in accordance with those of Milly et al. (2014; 2015), who used 45S5 powder in the form of a slurry and paste (mixed with polyacrylic acid) for 21 d (applied twice daily for 5 min) to enhance remineralization of demineralized human enamel surfaces, with or without adjunctive preconditioning (using air abrasion with the same glass). The protocol of the present study was simpler, less time-consuming, and therefore potentially of greater clinical appeal.

The surface characteristics of sound and demineralized enamel (via SEM) were similar to those reported in the literature (Dong et al. 2011; Ferrazzano et al. 2011; Jayarajan 2011; Gjorgievska et al. 2013; Milly et al. 2015). After glass (QMAT3) propulsion and immersion in AS to induce remineralization, SEM images showed mineral precipitations completely covering the enamel surface, suggesting that the bioactive glass particles were embedded in the treated enamel surface and effectively led to its remineralization. This occurred despite the teeth samples being rinsed with DW prior to imaging. These precipitations presented as dumbbell-like

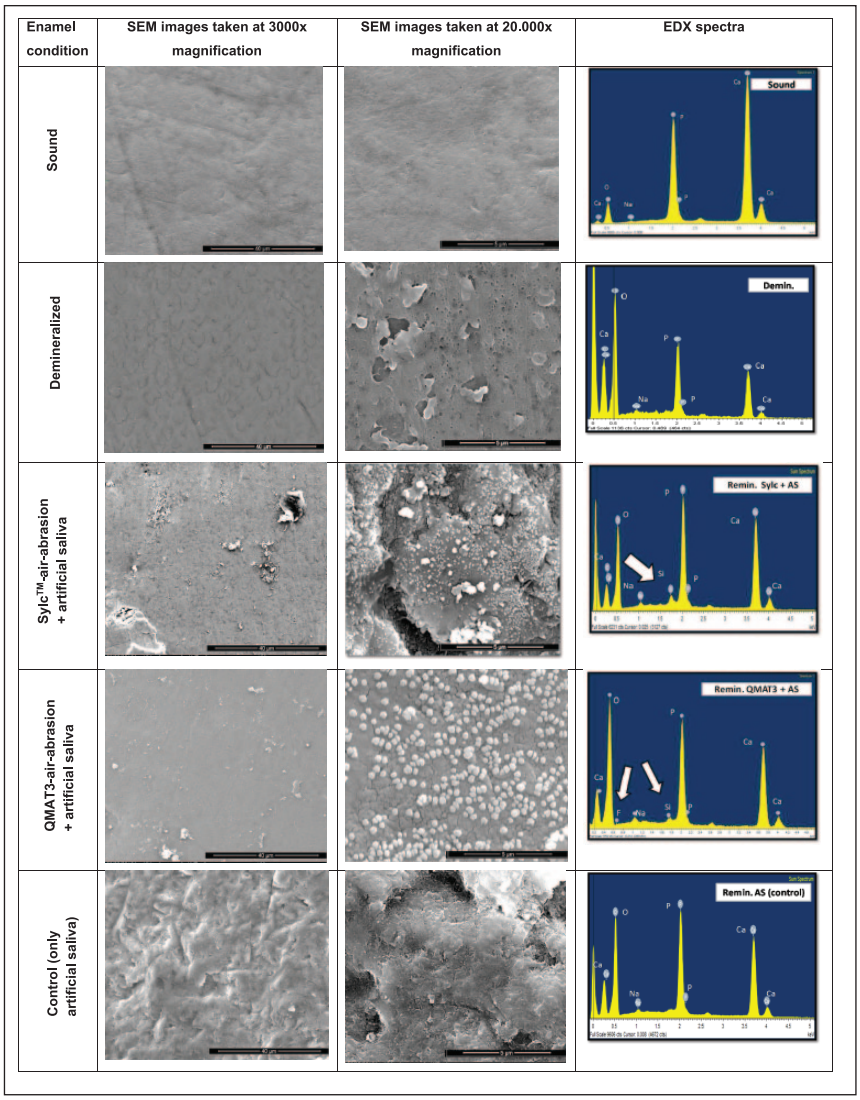

Figure 4. Scanning electron microscopy images and energy-dispersive X-ray spectroscopy spectra of enamel surface under 4 conditions. Arrows indicate the presence of silicon and fluoride peaks.

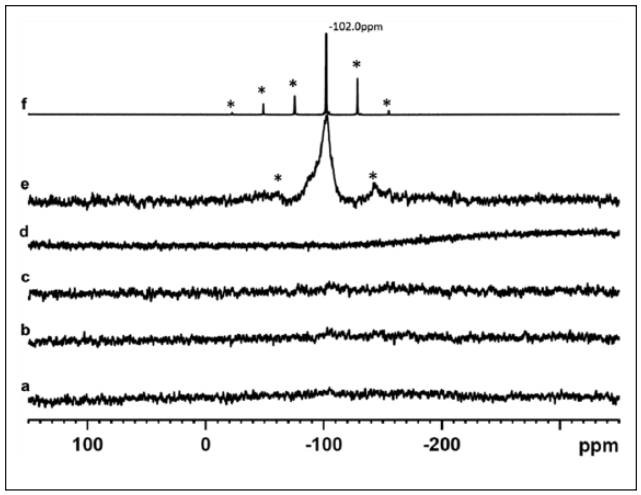

Figure 5. ^{19}F magic angle spinning–nuclear magnetic resonance spectra of enamel blocks under various conditions: (**a**) sound enamel; (**b**) demineralized enamel; (**c**) remineralized by only immersion in artificial saliva; (**d**) remineralized by propulsion with Sylc glass, followed by immersion in artificial saliva; (**e**) remineralized by propulsion with QMAT3 experimental glass, followed by immersion in artificial saliva; (**f**) fluorapatite reference. *Spinning side bands.

crystallites aggregated as a bunch of flowers; similar effects were reported in a number of studies where bioactive glass (45S5) was applied as a paste or slurry (Pulido et al. 2012; Gjorgievska et al. 2013; Bakry, Marghalani, et al. 2014; Bakry, Takahashi, et al. 2014; Milly et al. 2014; Narayana et al. 2014; Milly et al. 2015). However, these precipitations only partially filled the pores in the enamel surfaces propelled with Sylc, indicating that partial enamel remineralization occurred.

The EDX findings supported the appearance of the SEM images with the presence of an additional peak of Si after Sylc glass propulsion and 2 additional peaks for Si and fluoride after propulsion of experimental fluoride-containing QMAT3 glass. These peaks confirmed the incorporation of the glass particles within the enamel surface, which were not detected prior to propulsion of these glasses. This implies that the embedded particles resulted in apatite-like structures and did not simply represent deposits of nonreacted bioactive glass particles. The Si peak was an indication of the presence of silica gel formation, while the 2 Si and fluoride peaks (after QMAT3 propulsion) suggest the formation of silica gel and the possible formation of fluorapatite, although the latter was not proven definitively on this basis. Hence, the findings of OCT, noncontact profilometer, Knoop hardness testing, SEM, and EDX were consistent in suggesting the remineralization of WSLs after QMAT3–air abrasion and immersion in AS (24 h).

^{19}F MAS-NMR spectroscopy confirmed the presence of fluorapatite in remineralized enamel blocks after QMAT3–air abrasion alone. Similar findings with ^{19}F MAS-NMR were obtained by Mohammed et al. (2013), who studied the effect of immersion on demineralized enamel blocks in a remineralizing solution (0.1M acetic acid buffered with NaOH to pH 4) containing NaF of different concentrations. The authors found that fluorapatite was formed on these blocks after immersion (solution containing 11-ppm fluoride) for 96 h at 37 °C. Hill et al. (2015) also detected the formation of fluorapatite by ^{19}F MAS-NMR on demineralized enamel blocks after immersion for 96 h at 37 °C in a remineralizing solution (0.1M acetic acid, pH 4) containing a commercial mouthwash or a toothpaste (Ultradex, Perioducts Ltd; diluted to 10%). Both products contained nanohydroxyapatite powder (5% and 7.5%, respectively) and fluoride in the form of sodium monofluorophosphate (600 and 1,000 ppm, respectively). However, fluorapatite formed more efficiently in the current study (at 24 h, the end point of the experiment). It could be speculated that formation commenced earlier, as the glass dissolution studies (Taha et al. 2018) verified apatite presence at 6 h in Tris buffer and 30 min in AS.

QMAT3—the experimental glass with increased sodium and phosphate content, decreased silica content, and a constant level of fluoride—performed exceptionally well as compared with 45S5 or Sylc. The chemical composition led to increased dissolution rates and more rapid apatite formation in all immersion solutions. The high sodium content was shown to reduce the hardness of QMAT3, avoiding enamel damage on removal of residual orthodontic adhesive (Taha et al. 2018). Finally, the presence of a low level of fluoride at 3 mol% prevented the formation of unwanted fluorite and favored fluorapatite formation. The latter is particularly beneficial, since fluorapatite is more chemically stable than hydroxyapatite and is more resistant to acid attack associated with cariogenic bacteria, which might otherwise trigger enamel demineralization and WSL formation (Featherstone 2000; Robinson et al. 2000). Notwithstanding this, we acknowledge that we did not assess aesthetic changes associated with remineralization of WSLs in this ex vivo study; as such, the cosmetic impact of remineralization with bioactive glass remains unclear.

Conclusions

Based on these in vitro findings, the novel fluoride-containing QMAT3 glass was capable of enhancing enamel remineralization more effectively than a commercially available bioactive glass (Sylc), suggesting its potential utility in promoting WSL remineralization, as it formed fluorapatite when in contact with physiologic-like solutions. Further in vivo evaluation is required to confirm its clinical utility.

Author Contributions

A.A. Taha, contributed to conception, design, data acquisition, analysis, and interpretation, drafted and critically revised the manuscript; P.S. Fleming, R.G. Hill, M.P. Patel, contributed to conception, design, data analysis, and interpretation, drafted and critically revised the manuscript.

Acknowledgments

The authors thank Professor Sanjukta Deb and Richard Mallett, Tissue Engineering and Biophotonics Department in King's College London, Dental Institute, for allowing the use of their Knoop hardness testing instrument. They also extend their

gratitude to senior lecturer in dental biometrics Dr. Pete Tomlins for his expert assistance with OCT, senior lecturer Dr. Natalia Karpukhina, and the NMR facility manager in Queen Mary University of London, Dr. Harold Toms, for their expert technical assistance. This study is a part of a PhD that is being funded by the Iraqi Ministry of Higher Education and Scientific Research. The authors declare no potential conflicts of interest with respect to the authorship and/or publication of this article.

References

Bakry AS, Marghalani HY, Amin OA, Tagami J. 2014. The effect of a bioglass paste on enamel exposed to erosive challenge. J Dent. 42(11):1458–1463.

Bakry AS, Takahashi H, Otsuki M, Tagami J. 2014. Evaluation of new treatment for incipient enamel demineralization using 45S5 bioglass. Dent Mater. 30(3):314–320.

Beerens MW, Van Der Veen MH, Van Beek H, Ten Cate JM. 2010. Effects of casein phosphopeptide amorphous calcium fluoride phosphate paste on white spot lesions and dental plaque after orthodontic treatment: a 3-month follow-up. Eur J Oral Sci. 118(6):610–617.

Bröchner A, Christensen C, Kristensen B, Tranæus S, Karlsson L, Sonnesen L, Twetman S. 2011. Treatment of post-orthodontic white spot lesions with casein phosphopeptide-stabilised amorphous calcium phosphate. Clin Oral Invest. 15(3):369–373.

Chambers C, Stewart S, Su B, Sandy J, Ireland A. 2013. Prevention and treatment of demineralisation during fixed appliance therapy: a review of current methods and future applications. Br Dent J. 215(10):505–511.

Cochrane NJ, Anderson P, Davis GR, Adams GG, Stacey MA, Reynolds EC. 2012. An x-ray microtomographic study of natural white-spot enamel lesions. J Dent Res. 91(2):185–191.

Dong ZH, Chang J A, Zhou Y, Lin KL. 2011. In vitro remineralization of human dental enamel by bioactive glasses. J Mater Sci. 46(6):1591–1596.

Earl JS, Leary RK, Muller KH, Langford RM, Greenspan DC. 2010. Physical and chemical characterization of dentine surface following treatment with NovaMin technology. J Clin Dent. 22(3):62–67.

Featherstone JD. 2000. The science and practice of caries prevention. J Am Dent Assoc. 131(7):887–899.

Ferrazzano GF, Amato I, Cantile T, Sangianantoni G, Ingenito A. 2011. In vivo remineralizing effect of GC tooth mousse on early dental enamel lesions: SEM analysis. Int Dent J. 61(4):210–216.

Gjorgievska ES, Nicholson JW, Slipper IJ, Stevanovic MM. 2013. Remineralization of demineralized enamel by toothpastes: a scanning electron microscopy, energy dispersive x-ray analysis, and three dimensional stereo-micrographic study. Micros Microanal. 9(3):587–595.

Hill RG, Gillam DG, Chen X. 2015. The ability of a nano hydroxyapatite toothpaste and oral rinse containing fluoride to protect enamel during an acid challenge using 19 F solid state NMR spectroscopy. Mater Letters. 156:69–71.

Huang TT, Jones AS, He LH, Darendeliler MA, Swain MV. 2007. Characterisation of enamel white spot lesions using x-ray micro-tomography. J Dent. 35(9):737–743.

Jayarajan J, Janardhanam P, Jayakumar P, Deepika. 2011. Efficacy of CPP-ACP and CPP-ACPF on enamel remineralization—an in vitro study using scanning electron microscope and DIAGNOdent. Indian J Dent Res. 22(1):77–82.

Jones R, Fried D. 2006. Remineralization of enamel caries can decrease optical reflectivity. J Dent Res. 85(9):804–808.

Kang H, Darling CL, Fried D. 2012. Nondestructive monitoring of the repair of enamel artificial lesions by an acidic remineralization model using polarization-sensitive optical coherence tomography. Dent Mater. 28(5):488–494.

Lynch JM, Mony U, Ten Cate JM. 2007. Effect of lesion characteristics and mineralising solution type on enamel remineralisation in vitro. Caries Res. 41(4):257–262.

Magalhães AC, Moron BM, Comar LP, Wiegand A, Buchalla W, Buzalaf AR. 2009. Comparison of cross-sectional hardness and transverse microradiography of artificial carious enamel lesions induced by different demineralising solutions and gels. Caries Res. 43(6):474–483.

Mayne RJ, Cochrane NJ, Cai F, Woods MG, Reynolds EC. 2011. In-vitro study of the effect of casein phosphopeptide amorphous calcium fluoride phosphate on iatrogenic damage to enamel during orthodontic adhesive removal. Am J Orthod Dentofacial Orthop. 139(6):e543–e551.

Milly H, Festy F, Andiappan M, Watson TF, Thompson I, Banerjee A. 2015. Surface pre-conditioning with bioactive glass air-abrasion can enhance enamel white spot lesion remineralization. Dent Mater. 31(5):522–533.

Milly H, Festy F, Watson TF, Thompson I, Banerjee, A. 2014. Enamel white spot lesions can remineralise using bio-active glass and polyacrylic acid-modified bio-active glass powders. J Dent. 42(2):158–166.

Mneimne M. 2014. Development of bioactive glasses for dental treatment (Doctoral dissertation). London (UK): Queen Mary University of London.

Mohammed NR, Kent NW, Lynch RJM, Karpukhina N, Hill R, Anderson P. 2013. Effects of fluoride on in vitro enamel demineralization analyzed by 19F MAS-NMR. Caries Res. 47(5):421–428.

Narayana SS, Deepa VK, Ahamed S, Sathish ES, Meyappan R, Kumar KS. 2014. Remineralization efficiency of bioactive glass on artificially induced carious lesion an in-vitro study. J Indian Soc Pedod Prev Dent. 32(1):19–25.

Pulido R, Perdomo BJ, Pérez JP, Ramírez RA. 2012. Potencial de remineralización ultraestructural del vidrio bioactivo versus fluoruro estañoso. Acta Odontol. 50(4):4–8.

Robinson C, Shore RC, Brookes SJ, Strafford S, Wood SR, Kirkham J. 2000. The chemistry of enamel caries. Crit Rev Oral Biol Med. 11(4):481–495.

Sangamesh B, Kallury A. 2011. Iatrogenic effects of orthodontic treatment—review on white spot lesions. Int J Sci Eng Res. 2(5):2–16.

Silverstone LM, Wefel JS, Zimmerman BF, Clarkson BH, Featherstone MJ. 1981. RemineraIization of natural and artificial lesions in human dental enamel in vitro. Caries Res. 15(2):138–157.

Srivastava K, Tikku T, Khanna R, Sachan K. 2013. Risk factors and management of white spot lesions in orthodontics. J Orthod Sci. 2(2):43–49.

Taha AA, Hill RG, Fleming PS, and Patel MP. 2018. Development of a novel bioactive glass for air-abrasion to selectively remove orthodontic adhesives. Clin Oral Investig. 22(4):1839–1849.

Taha AA, Patel MP, Hill RG, Fleming PS. 2017. The effect of bioactive glasses on enamel remineralization: a systematic review. J Dent. 67:9–17.

Ten Cate JM, Exterkate RA, Buijs MJ. 2006. The relative efficacy of fluoride toothpastes assessed with pH cycling. Caries Res. 40(2):136–141.